Chapter 21
First Results of the Geotechnical In Situ Investigation for Soil Characterisation Along the Upper Slope Off Vesterålen: Northern Norway

Sylvia Stegmann, Stefan Kreiter, Jean-Sebastien L'Heureux, Maarten Vanneste, David Völker, Nicole Jeanne Baeten, Siren Knudsen, Leif Rise, Oddvar Longva, Jo Brendryen, Haflidi Haflidason, Shyam Chand, Tobias Mörz, and Achim Kopf

Abstract High-resolution geophysical data reveal the presence of several spatially-isolated, small-scale landslides along the gently dipping (~3–4°) upper slope off Vesterålen, Northern Norway. Dynamic slope stability analysis suggests that seismicity may be largely responsible for the occurrence of these slope failures. The landslides are clustered in two groups, with one group of parallel features with their headwalls in ~500 m water depths. The second group is found in ~800 m water depths.

We present first results of geotechnical *in situ* Cone Penetration Test (CPTU) data and TOPAS sub-bottom profiles collected during two cruises in summer 2013/2014. We obtained a total of six static CPTU profiles penetrating the top 20 m of soil. Three of these were taken across one of the landslide complexes (SL3) from the slide scar down to the depositional area. The other three are reference sites in the adjacent undisturbed areas.

The combination of geophysical and geotechnical data allows us to divide the well-stratified glacio-marine slope deposits into three different sediment-mechanical units, and reveals the occurrence of mechanically weaker zones (MWZ). These zones are interbedded by coarser layers with high values of cone

S. Stegmann (✉) • S. Kreiter • D. Völker • T. Mörz • A. Kopf
MARUM – Center for Marine and Environmental Sciences, University of Bremen, Bremen, Germany
e-mail: sstegmann@marum.de

J.-S. L'Heureux • M. Vanneste • S. Knudsen
Norwegian Geotechnical Institute (NGI), Oslo/Trondheim, Norway

N.J. Baeten • L. Rise • O. Longva • S. Chand
Geological Survey of Norway (NGU), Trondheim, Norway

J. Brendryen • H. Haflidason
Department of Earth Science, University of Bergen, Bergen, Norway

tip resistance. The occurrence of sensitive fine-grained material may be responsible for the loss of strength in the deeper portion.

One-dimensional pseudo-static stability analysis attests that the Vesterålen slope is stable except for exceptionally large earthquakes, that induce a peak-ground acceleration (PGA) of 0.224 g or larger to the MWZ. The depth levels of the MWZ correspond well with the slide planes of the landslides.

21.1 Landslides Along the Slope Off Vesterålen

Landslide processes off the Norwegian margin are abundant, with the Storegga Slide being the most prominent example (e.g. Haflidason et al. 2004). In this study, we focus on clusters of small-scale landslide features on the gently dipping slope (~3–4°) off Vesterålen, Northern Norway (Fig. 21.1). The landslides in one cluster
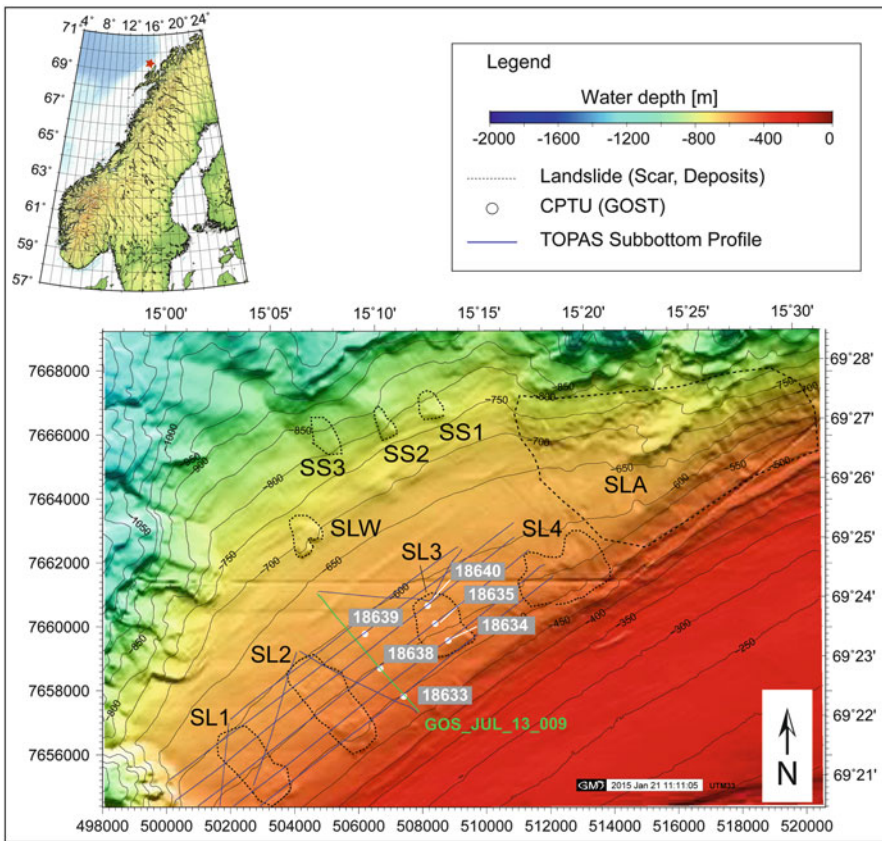

Fig. 21.1 Bathymetric map of the study area on the gently dipping slope off Vesterålen (www.mareano.no). Isolated slope failure features are aligned parallel along 500 and 800 isobath

have their headwalls at around the 500 m isobaths, whereas the second cluster is located in slightly deeper water areas. The spatially-isolated landslides occur in an area essentially devoid of topographic relief and disconnected from both canyon systems and the glacial termini further upslope (Laberg et al. 2007). The volume of failed material varies between $8.5 \cdot 10^6$ and $16.0 \cdot 10^6$ m^3. The run-out distances of these landslides do not exceed 3350 m (L'Heureux et al. 2013). The landslides (SL1-SL4, SLA, SLW) cut the slope-parallel stratified glacio-marine silty to sandy clays on two well-defined slide planes (Rise et al. 2012). The sliding surfaces coincide with spatially continuous high-amplitude reflections (Rise et al. 2012; L'Heureux et al. 2013, Fig. 21.3, horizons a and c). It is unclear, however, whether the sliding planes of the slides are different in composition or have happened at the same time or not. Based on an already existing multidisciplinary database (see Vanneste et al. 2014), the soils consist of predominantly normally consolidated clays to silty clays with intermediate plasticity. Triaxial test results show intervals with strain-softening behaviour. A comprehensive slope stability assessment by L'Heureux et al. (2013) (i) attests that the slope is *per se* stable under static conditions and (ii) indicates that external seismically induced load and post-seismic pore pressure accumulation are the most relevant triggers for landslide and deformation processes.

21.2   Methods

21.2.1   Sub-bottom Mapping

In addition to the first sub-bottom mapping in 2010 (Rise et al. 2012), a complementary survey in summer 2013 was acquired using a parametric sub-bottom profiler system (TOPAS PS18) operated from R/V G.O. Sars (Univ. Bergen). Focus of the survey was set on the mapping of the landslide complexes SL1–SL4 (Fig. 21.1; Haflidason et al. 2010).

21.2.2   CPTU Investigation of Slope Sediments

During the cruise POS472 (MARUM/Univ. Bremen) with R/V Poseidon, geotechnical *in situ* data were collected using the high-resolution static **G**eotechnical **O**ffshore **S**eabed **T**ool (GOST) developed at MARUM. The system is equipped with a 5 cm^2 electrical piezocone with a pore pressure port (CPTU). After landing the GOST on the seafloor, the probe is pushed hydraulically with a constant velocity of 2 cm/s into the sediments. Cone resistance q_c, sleeve friction f_s and excess pore water pressure response Δu_2 are recorded with a sampling frequency of ~30 Hz, which results in a vertical resolution of ~2 mm. Excess pore water pressure is

measured differentially against the water filled rod directly behind the cone in u_2 location. For further details, see Jorat et al. (2014).

Processing of the CPTU data and the derivation of strength properties was accomplished according to standard practice summarized in Lunne et al. (1997). Undrained shear strength s_u was calculated using the static cone factor $N_{kt} = 12$, 15 and 17 for normally consolidated clayey sediments (Lunne et al. 1997). The normalised undrained shear strength (s_u/σ'_{v0}) can be used to determine the state of consolidation. For normally-consolidated soil, this ratio typically falls in the range of 0.2–0.3 (Karlsson and Viberg 1967). A ratio exceeding 0.3 may indicate overconsolidation.

Identification of soil types was carried out following the soil behaviour type classification by Ramsey (2002; SBT_{Ramsey}) and Robertson (1990; $SBT_{Robertson}$) using the normalised cone resistance Q_t $[(q_t - \sigma_{vo})/\sigma'_{vo}]$ and the pore pressure parameter B_q $[\Delta u_2/(q_t - \sigma_{vo})]$ with the vertical total stress (σ_{vo}) and the effective vertical stress (σ'_{vo}) (Lunne et al. 1997).

21.2.3 Pseudo-static Factor of Safety (FoS)

The 1D undrained, infinite slope stability analysis by Morgenstern and Price (1965) defines the pseudo-static factor of safety (FoS) – the ratio of resisting forces to driving forces during earthquake shaking. Seismic-induced shear stresses are considered to be constant over the period of shaking (Hampton et al. 1996). If FoS >1, the sediments are assumed to be stable. FoS <1 indicates permanent deformation and/or failure.

FoS is defined as

$$FoS = \frac{s_u}{\sigma'_{v0} \left(\sin(\alpha)\cos(\alpha) + k\left(\frac{\gamma}{\gamma'}\right)\cos^2(\alpha) \right)}$$

with α = the slope angle, γ' = the effective unit weight and the seismic coefficient k. Given the fact that soil slopes are not rigid and the peak ground acceleration (PGA) lasts for a very short period of time, seismic coefficients used in practice correspond to lower PGA values (Kramer 1996). Here, k was calculated with $0.3 \cdot$ PGA [g] recommended by Marcuson (1981) and following the proposition by Hynes-Griffin and Franklin (1984): $k = 0.5 \cdot$ PGA [g]. The latter criteria is suggested to be appropriate for most slopes by Kramer (1996).

We run the analysis using a PGA of 0.051 g and 0.224 g. These values correspond to potential seismic events offshore Vesterålen with a 90 % probability of no exceedance for 475 years and 10,000 years recurrence period, respectively (NORSAR 1998).

21.3   Results

Geophysical as well as *in situ* geotechnical CPTU data presented here (Figs. 21.2 and 21.3) focus on the characterization of the uppermost strata of the slope in terms of sediment-mechanical properties and slope stability (Fig. 21.1).

The TOPAS data illustrate that the sediments are well stratified with continuous strata packages of different reflectivity (Fig. 21.2). The scars of the different slide complexes clearly cut the slope sediments and terminate at different levels, typically on spatially-continuous reflections. Since the new TOPAS data closely resemble those presented by L'Heureux et al. (2013), we refrain from showing them here.

The CPTU penetrated between 7 and 19.8 m and profiled (i) intact material (GeoB18633, −38, −39) (Fig. 21.2) and (ii) different morphological parts of SL3 (GeoB18634, −35, −40) (Fig. 21.1) The CPTU located upslope (GeoB18633, −34) were stopped at 7 m and 9 m, when q_c reached 20 MPa and 44 MPa, respectively to avoid bending or breaking of the rods. Availability of reliable f_s data is limited as the sleeve friction jacket was blocked during some measurements.

21.3.1   *Sedimentological and Geotechnical Characterisation of Slope Sediments*

The correlation of geophysical and *in situ* CPTU data identifies three different sediment-mechanical units in the upper 20 m of slope sediments (Fig. 21.3).

Unit I has a well pronounced slope-parallel, distinct reflection pattern, in which corrected cone resistance q_t reaches peaks up to 0.93 MPa. Excess pore pressure Δu_2 rises up to 0.12 MPa. q_t of the background sediment increases linearly to
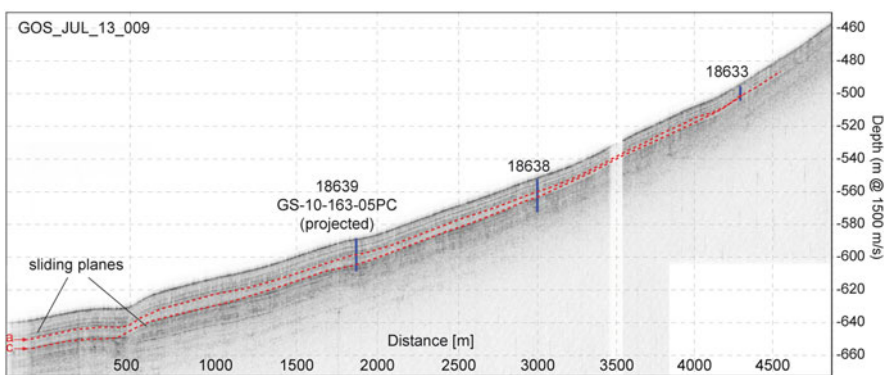

Fig. 21.2 Sub-bottom TOPAS profile crossing the location of the CPTU transect along the intact portion of the slope. Location of the seismic profile is shown in Fig. 21.1. Position as well as penetration of three CPTU are illustrated by *blue lines*. *Dashed red lines* represent the sliding planes according to Rise et al. (2012) and L'Heureux et al. (2013)
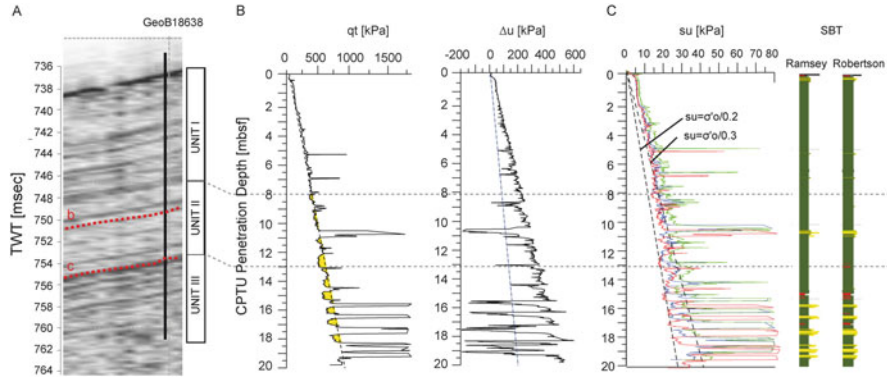
Fig. 21.3 Sediment-mechanical characterisation of intact slope sediments: (**a**) Position and penetration depth of GeoB18638 on the TOPAS line GOS_13_JUL_009; (**b**) *Yellow-shaded* areas indicate mechanically weaker zones (MWZ). (**c**) Undrained shear strength s_u was calculated with $N_{kt} = 12$ (*green*),15 (*black*) and 17 (*red*). *Dashed lines* are indicative of the state of consolidation based on s_u/σ'_{vo}. Soil behaviour types were determined by Robertson (1990) and Ramsey (2002). Colour-coding of the soil types: *green* = Clay, NC (Ramsey), silty clay (Robertson), *yellow*: silty sand to sand, *red*: sensitive fine-grained material. Please note that the CPTU and s_u data are clipped for better illustration

0.35 MPa, which corresponds to s_u of 18 kPa (Fig. 21.3c). With the normalized undrained shear strength up to 0.45 (based on s_u with $N_{kt} = 15$), the sediments appear slightly overconsolidated.

The reflections within Unit II appear less coherent than those of Unit I. A locally distributed coarse layer is detected between 10.5 m and 11 m with a peak in q_t reaching 12 MPa. A peak of that order does not appear in GeoB18639. The linear trend of s_u is decreasing marginally and approaches values typical for normally consolidated sediments (Fig. 21.3c). Immediately underneath the distinct peaks of q_t we find intervals with exceptional low q_t. These mechanically weaker zones (MWZ) are shaded in yellow in Fig. 21.3b.

Unit III is characterized by the alteration of coarse layers (high q_t and low Δu_2 values) with relative weaker zones (q_t values = 0.58 MPa, Fig. 21.3b). In this unit, again the geophysical data reveal clearly accentuated slope-parallel layering, s_u of MWZ decreases to 23 kPa minimum. The material is normally consolidated (Fig. 21.3c).

Excess pore pressure response Δu_2 increases linearly with depth to 330 kPa. Δu_2 lows coincide with q_t-peaks, which corresponds to dilative behaviour induced by shearing of the penetrating cone in coarser-grained material.

Two different types of soil type behaviour classification were used (SBT_{Ramsey}, $SBT_{Robertson}$) to characterize the thin-layered strata with q_t-values >1500 kPa as sandy layers. The background sediment is characterized by SBT_{Ramsey} as normally consolidated clay and by $SBT_{Robertson}$ as silty clay. Based on SBT the MWZ in Unit II and III correspond partly to sensitive fine-grained material (Fig. 21.3c).

Fig. 21.4 FoS was calculated for the CPTU profile GeoB18638. The *lower* boundary represents the FoS calculated with k = 0.5 * PGA [g], the *upper* boundary relates to k = 0.3 * PGA [g]. Slope angle α is 3°. s_u derived with N_{kt} = 15 was used for the calculation of FoS with a PGA of 0.224 g (10,000-years recurrence period). The *black line* represents the FoS related to a PGA = 0.051 g (475-years recurrence period). *Yellow-shaded* portions correlate to MWZ (see Fig. 21.3)
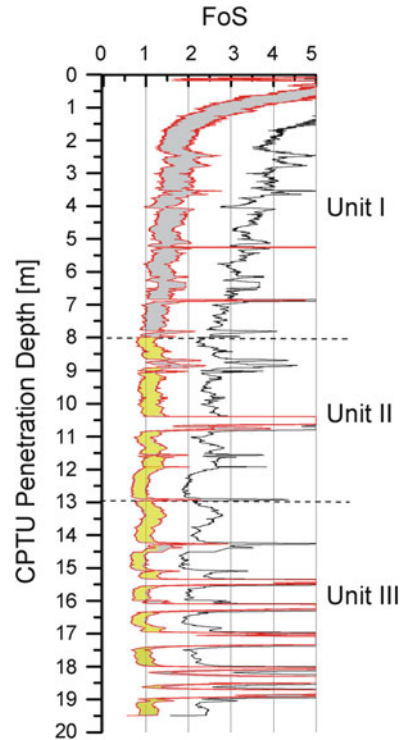
21.3.2 Pseudo-static Slope Stability Analysis

Results of the FoS analysis show that the PGA of the seismic event with 475 years-recurrence time (PGA = 0.051 g) is not sufficient to destabilize the slope sediment in any depth level (FoS >2; Fig. 21.4). When assuming an earthquake with a PGA of 0.224 g (i.e. 10,000 year return period event) the FoS comes close to 1 (meta-stable) or falls below unity within the sediment-mechanical Unit II and III for cases where s_u is estimated with N_{kt} = 15, respectively. These failure depths correlate to the MWZ identified by means of CPTU tests in Fig.21.3b.

21.4   Discussion and Outlook

Along the stable slope offshore Vesterålen, static CPTU data reveal the occurrence of mechanically weaker zones (MWZ) by the drop of q_t-values (Fig. 21.3b). Within the sediment-mechanical Unit III, some MWZ coincide with layers where sensitive fine-grained sediments were classified by $SBT_{Robertson}$ and SBT_{Ramsey} (Fig. 21.3; Units II, III).

   The 1D infinite, undrained pseudo-static stability calculation presents several critical slope layers (meta-stable to unstable) in Unit II and III, indicating

permanent deformation or failure in case additional dynamic load is induced by an earthquake (Fig. 21.4). According to L'Heureux et al. (2013), a 10,000 year-seismic event with a PGA of 0.224 g is necessary to produce failure or permanent deformation along the slope. Such seismic events, which historically had magnitude M5.7 may have been frequent due to the glacio-isostatic uplift after the last glaciation along the slope off Vesteralen (Bungum et al. 1991; Olesen et al. 2013).

Given the fact that the stability analysis does not account for earthquake-induced excess pore pressure and inherent shear strength reduction due to accumulation of deformation, this undrained pseudo-static analysis is only a first-order approximation providing a relative stability index for the upper slope sediments. The seismic reflectors b and c (Figs. 21.2 and 21.3a) represent the sliding surfaces for SL1-SL4 and SLA, respectively (L'Heureux et al. 2013; Rise et al. 2012). The results of our analysis reveals the occurrence of critical layers, which correspond to reflector b (~10 mbsf) and c (~13 mbsf) (Fig. 21.4). The analysis attests that the mechanically weaker zones (MWZ) correlate well with the portions where FoS ≤1 (Fig. 21.4). Thus, the mechanically weak layers can be considered as one important pre-condition for landslide activity along the gently dipping slope. External trigger (e.g. large magnitude seismic event), however, is necessary to generate landslide activity along the slope off Vesterålen.

In conclusion, the integration of *in situ* CPTU data with geophysical data improves soil characterization and hence foster a better understanding of the pre-conditioning factors for slope instability at the upper continental slope off Vesterålen.

Based on these preliminary *in situ* CPTU data, further (2D) analysis is necessary to understand i) the liquefaction potential of the coarse-grained layers and ii) the influence of the stratified fine-grained – sandy sequence in Unit III on the dissipation behaviour of seismic-induced excess pore pressure, and iii) the factors, which control the stability of the RWZ in deeper portion (13 m–18 m, Unit III; Fig. 21.4). Risk assessment for the present-day slope requires these studies for the slope off Vesterålen, where the opening for offshore oil and gas exploration is controversially debated (Misund and Olsen 2013).

References

Bungum H, Alsaker A, Kvamme LB, Hansen RA (1991) Seismicity and seismotectonics of Norway and surrounding continental shelf areas. J Geophys Res 96:2249–2265
Haflidason H et al (2004) The Storegga Slide: architecture, geometry and slide-development. Mar Geol 213:201–234

Haflidason H et al (2010) Marine geological cruise report from mid-Norwegian continental shelf, Ranafjorden-Sørfjorden and Lofoten-Vesterålen margin. Report No. 100-02/10, Department of Earth Science, University of Bergen, Bergen, 39 pp

Hampton MA, Lee HJ, Locat J (1996) Submarine landslides. Rev Geophys 34(1):33–59

Hynes-Griffin ME, Franklin AG (1984) Rationalizing the seismic coefficient method. Miscellaneous Paper GL-84-13, US Army Corps of Engineers, Vicksburg

Jorat ME, Moerz T, Schunn W, and Kreiter S (2014) Geotechnical offshore seabed tool (GOST): a new cone penetrometer, In: Robertson PK, Cabal KL (eds) CPT'14. procs. 3rd intern. symp. on cone penetration testing, CPT'14 Organizing Comittee, Las Vegas, pp 207–215

Karlsson R, Viberg L (1967) Ratio of c/p in relation to liquide limit and plasticity index, with special reference to Swedish clays. In: Proceedings, conference on shear strength properties of natural soils and rocks, vol 1. Oslo

Kramer SL (1996) Geotechnical earthquake engineering. Prentice Hall, Upper Saddle River

L'Heureux JS et al (2013) Stability, mobility and failure mechanism for landslide at the upper continental slope off Vesteralen, Norway. Mar Geol 346:192–207

Laberg JS, Guidard S, Mienert J, Vorren TO, Haflidason H, Nygård A (2007) Morphology and morphogenesis of a high-latitude canyon area; the Andøya Canyon, Norwegian Sea. Mar Geol 246:68–85

Lunne T, Robertson PK, Powell JJM (1997) Cone penetration testing in geotechnical practice. Spon Press, London

Marcuson WF (1981) Modeator's report for session on "Earth dams and stability of slopes under dynamic loads". Proccs, Intern Conference on Recent Advances in Geotechnical Earthquake Engineering and Soil Dynamics, St. Louis, Vol 3, 1175

Misund OA, Olsen E (2013) Lofoten–Vesteralen: for cod and cod fisheries, but not foroil? ICES J Mar Sci. doi:10.1093/icesjms/fst086

Morgenstern NR, Price VE (1965) Analysis of stability of general slip surfaces. Geotechnique 15(1):79–93

NORSAR (1998) Development of a seismic zonation for Norway. Norwegian Council for Building Standardization (NBR), p 162

Olesen O, Bungum H, Dehls J, Lindholm C, Pascal C, Roberts D (2013) Neotectonics, seismicity and contemporary stress field in Norway – mechanisms and implications. In: Olsen L, Fredin O, Olesen O (eds) Quaternary geology of Norway, vol 13, Geological survey of Norway special publication., pp 145–174

Ramsey N (2002) A calibrated model for the interpretation of cone penetration tests (Cpts) in north sea quaternary soils. Offshore site investigation and geotechnics 'Diversity and Sustainability'; Proceedings of an international conference, 26–28 Nov, London

Rise L et al (2012) Investigations of slides at the upper continental slope off Vesterålen, North Norway. In: Yamada Y, Kawamura K, Ikehara K, Ogawa Y, Urgeles R, Mosher DC, Chaytor J, Strasser M (eds) Submarine mass movements and their consequences (5th international symposium). Springer Netherlands, pp 167–176

Robertson PK (1990) Soil classification using the cone penetration test. Can Geotech J J 27(1):151–158

Vanneste M et al (2014) Seafloor instabilities and sediment deformation processes: the need for integrated, multidisciplinary investigations. Mar Geol. doi:10.1016/j.margeo.2014.01.005